Influence of topography on ground deformation at Mt. Vesuvius (Italy) by finite element modelling

M. Meo, U. Tammaro, P. Capuano

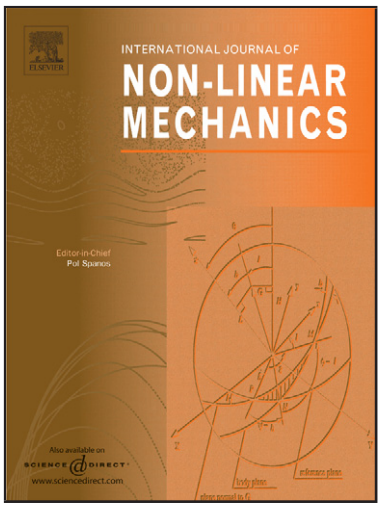

www.elsevier.com/locate/nlm

Influence of topography on ground deformation at Mt. Vesuvius (Italy) by finite element modelling

M. Meo, U. Tammaro, P. Capuano

PII: S0020-7462(07)00228-4
DOI: doi:10.1016/j.ijnonlinmec.2007.12.005
Reference: NLM 1422

To appear in: *International Journal of Non-Linear Mechanics*

Received date: 25 May 2007
Revised date: 10 December 2007
Accepted date: 11 December 2007

Cite this article as: M. Meo, U. Tammaro and P. Capuano, Influence of topography on ground deformation at Mt. Vesuvius (Italy) by finite element modelling, *International Journal of Non-Linear Mechanics* (2007), doi:10.1016/j.ijnonlinmec.2007.12.005

Influence of topography on ground deformation at Mt. Vesuvius (Italy) by finite element modelling

M. Meo[1], U. Tammaro[2], P. Capuano[3,2]

[1] Department of Mechanical Engineering, University of Bath, BA2 7AY, UK
[2] Istituto Nazionale di Geofisica e Vulcanologia, sezione Osservatorio Vesuviano, Naples, Italy
[3] Dipartimento di Matematica e Informatica, University of Salerno, Fisciano (SA), Italy

Abstract

Ground deformations are observed in connection with volcanic activity, and therefore geodetic monitoring can provide significant indication of changes of equilibrium conditions. The aim of this paper is to study the deformation of Mount Vesuvius (Italy) caused by overpressure sources at various depths, using a commercial (Ansys) 3D finite element code, in the framework of linear elastic isotropic material behaviour. Both homogenous and heterogeneous media with carbonate basement were analyzed to understand the influence of topography on the ground deformations. The topography of the Somma-Vesuvius was taken into account, using a digital terrain model, and the carbonate basement was schematically modelled by assuming two horizontal layers with different Young moduli. The presence of a strong deviation from axially symmetric pattern of the displacement field, and of small subsidence areas, was found. These characteristics are completely unknown from the simple Mogi model and by simplified topography model, as verified by *ad hoc* simulations. These preliminary results, showing areas of the volcanic edifice experiencing high deformation, can improve the determination of the sources of deformations, i.e. the most relevant problem in the volcano monitoring. Moreover, the knowledge of the deformation pattern, including the topography effects, can provide significant indications to optimize the

location of sensors and the characteristics needed to design an efficient and reliable geodetic monitoring network able to detect shallow intrusion events.

1. Introduction

During almost three centuries Mt. Vesuvius has been the natural laboratory where scientists came from all over the world to test theories and to experiment new methods. Mt. Vesuvius has been quiescent since 1944. Since then an uncontrolled expansion of the municipalities located on the slope of the volcano occurred; thus the dense population surrounding it and its slopes became the most notable aspect of Vesuvius among Earth's volcanoes. However, Vesuvius is a very dangerous volcano, in fact, its volcano's history suggests that the longer is the quiescence period, the more violent is the renewal of activity. This has transformed Mt. Vesuvius surroundings into an area with the highest volcanic risk in the world.

The Somma-Vesuvius (Fig. 1) is a volcano located within a graben (Campanian Plain) formed in Plio-Pleistocene. It is made by an older stratovolcano (Mt. Somma) with a summit caldera partially filled by the composite younger cone of Mt. Vesuvius. The Campanian Plain is bordered by mostly Mesozoic carbonate rocks. During the last 20 ky seven Plinian eruptions occurred. The last one is the famous "Pompeii" eruption which occurred in 79 A.D. After this eruption three sub-plinian eruption occurred (472, 512, 1631 A.D.). From 1638 to 1944 Mt.Vesuvius was in an almost continuous strombolian activity with occasionally moderate explosive eruptions. Since 1944, Mt. Vesuvius entered a quiescence stage, which is presently characterized by moderate low magnitude seismicity (up to M_D = 3.6, recorded on October 1999), low temperature fumaroles at the summit crater and the absence of ground deformation.

For this reason, Mt. Vesuvius is carefully monitored. A 3-D model of the shallow structures of the volcano and an optimized monitoring network would allow a better definition of the characteristics of the precursors of eruptions, through a substantial improvement of the accuracy of location of seismic and ground deformation sources.

Recently, strong efforts have been devoted to the definition of its structure and the location of magma reservoir, with the objective to help prediction of the scenario of the next eruption and to interpret the pattern of the expected precursory signals. A number of geophysical studies have been performed in the framework of a seismic tomography project, called TomoVes [*Capuano et al.,* 2003]. The main results of this project are detailed images of the shallow volcanic structure and the Campanian Plain [*Zollo et al.,* 1996*; Di Stefano and Chiarabba,* 2002*; De Natale et al.,* 2004] and evidence for a 8 to 10 km deep midcrustal discontinuity associated with an extended molten or partially molten zone [*Auger et al.,* 2001]. This low velocity zone (at least 400 km^2) was interpreted as a large scale series of sills below the volcano edifice, with magma interspersed in a solid matrix, extending toward East and in the direction of the near volcanic centre of Campi Flegrei, covering a volume larger than $500k^3$. Analysis of fluid inclusion in phenocrysts provides information about the lithostatic pressure under which the Vesuvius magmas crystallize. Application of these methods to the last eruptions of Vesuvius (1906 and 1944) suggests the presence of magma reservoir at shallow depth (2-5km), refilled during the eruptions by magma coming from a deeper (10-20km) reservoir (*Fulignati et al.,* 2000). Fluid inclusions in older Vesuvius products indicate crystallization depth between 4 and 10 km (*Belkin et al.,* 1993).

A 3D velocity model of the Mt. Vesuvius area have been reconstructed by *Lomax et al.* [2001] to estimate earthquake location and fault mechanism. The main feature of this model is the complex shape of the carbonate basement surface.

In order to detect in advance significant variations in some parameters which can indicate reactivation, Vesuvius is monitored by a comprehensive system of seismic, geodetic and geochemical networks managed by the Osservatorio Vesuviano. One of the main problems in volcano monitoring is how design an optimal monitoring network to be able to detect weak precursory signals, generated by the interrelationship between sources, structures including topography and sensors. Thus, in order to investigate how the complex structure of a volcano can affect the deformation field, more realistic simulations are of vital importance to improve the

determination of the sources of surface deformations and to find optimal measurement sites location.

The effects of topography on the deformation field have been presented in many papers showing that the mechanical model of volcano [*Mogi,* 1958] were unsuccessful in the estimation of ground deformations because of the assumption of flat topography and half space solutions. In particular, *McTigue and Segall* [1988], investigated the effects of topography on surface displacements by using a plane-symmetric approximation. *Cayol and Cornet* [1998] considered an axial symmetrical volcano with average slopes of flanks ranging from 0° to 30° and they showed that the flattening of the deflation in the summit area is probably a topographic effect: the steeper the volcano, the lower the central uplift. *Williams and Wadge* [1998] showed that the predicted deformation field varies significantly when topography is included.

Trasatti et al. [2003] investigated the effects of topography and rheological layering on ground deformation at Mount Etna, by assuming the approximate topography as axial symmetrical. They showed, in agreement with results of *Cayol and Cornet* [1998], the existence, on the topography surface, of an annular region of maximum uplift with a central depression.

Russo and Giberti [2004] developed 3D asymmetric and 2D axisymmetric finite element numerical models with heterogeneities of country rocks at Mt. Vesuvius. Their model took into account the presence of volcanic edifice: the volcanic structure was axially symmetric with a summit at about 1200 m above sea level and flanks drop to sea over 7 km.

Finally, *Lungarini et al.* [2005] analyzed topographic effects on elastic ground deformation at Mount Etna with a model that use the real 3D topography of volcano. Their work showed, through the comparison of FEM and half-space models results, the importance of using a full 3D topography when studying ground deformation at volcanoes.

All the cited papers showed that real 3D topography can produce significant effects on the ground deformation pattern in the case of central volcanos with strong slopes of their flanks. In this paper, we calculated the ground deformation patterns of Vesuvius surface due to an overpressure

source at various depths, by developing for the first time a full 3D finite element model based on the real topography. This model can be used for the detection of the sources of deformations and for the design of an optimal geodetic monitoring network.

2. Seismic tomography investigations

The idea of realizing a high resolution seismic experiment on Mt. Vesuvius was driven by the need of a detailed reconstruction of the volcano structure, including the location and size of the magmatic reservoir(s), in order to predict quantitatively the possible scenarios of the next eruption. Although a hundred local microseismic (M_D < 3.6) events occur in average every year at Mt. Vesuvius, most of them are located in a clustered area just below the crater and they are shallower than 4 km making the passive tomography approach unfruitful. Then, the proposed project relied mostly on active energy sources.

During TomoVes experiment, five multi-two-dimensional profiles (Fig. 1) were analysed with a total of 17 shot points, recorded by about 140 3-component seismographs. Seismic signals of each shot were recorded simultaneously along the longitudinal and quasi-orthogonal directions (for more details see Gasparini et al., 1998).

Firstly, a 1D non linear inversion τ-p method approximating the Earth's topography with spherical shells and including body waves was performed (De Matteis et al., 2000) to provide a reliable 2D initial model for perturbative tomography inversion. The choice of a non-linear approach, instead of a linearized tomography inversion was due to the strong heterogeneity of the investigated medium that make the definition of a reliable initial velocity model challenging, despite of the availability of subsurface information. In this case, a linearized approach may fail if the used *a priori* reference velocity model is too far from the actual velocity structure.

In particular, a Bayesian approach (Zollo et al., 2002) to image the shallow structure of Mt Vesuvius volcano and the surrounding plain was developed. The problem of velocity field estimation was solved through the computation, during the model space exploration, of the *a*

posteriori probability density function (pdf) which relates the observed to predicted arrival time data. In this way, a maximum likelihood velocity model was obtained, which is particularly useful for mapping errors on parameters and for selecting the optimal medium parameterization. The latter was evaluated by applying the Akaike Information Criterion (Akaike 1974) which takes into account the concepts of best misfit and simplicity of the model (small number of parameters). The search for the maximum likelihood model, maximizing the pdf, in the multidimensional parameter space was performed by a non-linear optimization method which uses, at consecutive steps, the Genetic (Goldberg 1989) and Simplex (Press *et al.* 1986) algorithms. A 'multi-scale' approach was used. This procedure, which was introduced for velocity estimation by Lutter *et al.* (1990), allowed us to determine the large-scale components of the velocity model and to estimate progressively the smaller-scale components. This is roughly equivalent to moving from a low to high wavenumber description of the velocity field. The cubic spline was used to compute the velocity values at every point of the 2D gridded medium. The cost function used in the inversion was a least-squares L_2 norm, defined as the sum of the weighted squared differences between observed and computed travel times.

Fig. 2 shows 2D tomography images relative to the 5 analyzed profiles. The inferred images show a high variability in the shallow structure, with values ranging from 1.5 km/s to 6 km/s, with a very sharp increase observed at depth ranging from few hundreds meters to 3-4 km. It was reasonably assumed that the top of the limestone formation is marked by the P-velocity isoline at 5000 m/s. The checkerboard analysis of the retrieved images shows that the best resolved areas are located beneath the volcanic complex.

Using a circumferential interpolation procedure a 3D P-velocity model and the topography of the top of the limestone basement were computed (Lomax et al., 2001). This model was used to refine earthquake location occurred in the Vesuvius area, using a non-linear global search location, using the probabilistic inversion presented by Tarantola and Valette (1982).

Finally, tomography studies (Capuano et al., 2003) revealed the absence of low velocity zone compatible with magma reservoirs up to 5-6 km depth, with a lateral resolution of approximately 0.5km. Based on this results and with the findings of a low velocity zone at 8-10km depth, as the possible primary source of the shallower magma chamber, we simulated overpressure source located at 2, 3, 5 km bsl with a lateral extension smaller than 0.5km, using reservoirs with a parallelepiped shape.

3. FEM model

A 3D linear-elastic finite element model to study ground deformation at Mt. Somma-Vesuvius was developed, using ANSYS commercial code. The validity of this approach is related to the time scale of the event we want to simulate. In general, the time scale of overpressure in magma chamber is much smaller than the scale of material relaxation in a volcano. Our model was built taking into account real topography of the volcano as inferred from a detailed digital elevation model. When modelling the behaviour of large scale structures such a volcano, various modelling issue must be taken into account. To describe a volume, either hexahedral or tetrahedral shaped can often be used; however, a combination of the two elements is not generally recommended. In our studies the choice of using hexahedral instead tetrahedral elements was dictated by higher accuracy and performance of these elements. The hexahedral element used was defined by eight nodes having three degrees of freedom at each node: translations in the all nodal directions.

One of the most important modelling issues is the assessment of the appropriate mesh density. Using a coarse mesh can generate inaccurate results. On the other hand, using a fine mesh leads to an increase of run times. To avoid such problems, in our work a sensitivity analysis of the appropriate mesh density was performed.

Another issue for a correct analysis was the level of details necessary to describe adequately the structural behaviour of the volcano. The mesh was constructed by using elements with smaller edge length in regions of high stress gradient while a coarser mesh was used away from the main

crater. In the main area of interest (with a side of 10 km) enclosing the volcano, brick elements with an edge length of 80 m were used; then a coarser mesh was used for the remaining domain with elements having a decreasing (maximum) edge length of 240 and 480 m. The final model was composed of 643525 nodes and 612880 elements.

The size of the domain is clearly a function of the loading conditions. In our case, various dimensions were considered for the various loadings considered to avoid edge effect. The domain size was chosen in such a way that no significant changes of the vertical displacement in volcano area were recorded for the loads imposed. Domain size was increased until nearly identical results for succeeding meshes were obtained. A tolerance of 5% was chosen between two different domain sizes. Finally, the model size is 37000x26000 m with a depth size of 25000 m (Fig. 3).

Regarding the boundary conditions, different constraints were imposed on the faces of the domain (Tab. 1).

A Pre-conditioned Conjugate Gradient iterative equation solver was used to perform the linear static analysis due to the reduced disk file space needed compared to other solvers and for its speed in solving large scale models. Sensitivity analysis of solver tolerance value was conducted and a value of $1.0 \cdot 10^{-6}$ was used.

Our objective is the computation, using a FEM approach, of the ground deformation at Vesuvius volcano, evidencing the strong influence on the deformation pattern due to the real complex topographic structure. Three different overpressure sources were considered located at various depths, 2, 3 and 5 km in a homogenous medium and in heterogeneous medium with carbonate basement. In particular, two half-space models to compute deformation at surface were used: a) an homogeneous model where the reservoir was represented by a prolate overpressure source parallelepiped shaped with a horizontal side of 480 m and thickness of 1.8 and 2.0 km, for the shallow and deeper source respectively, locate along the crater axis; b) an heterogeneous model schematically obtained assuming two horizontal different layers, the first underneath the crater and down to 2 km below sea level with Young's modulus equal to 10 GPa and the second layer,

representing the carbonate basement, with a Young's modulus of 40 GPa (Russo and Giberti, 2004). The Poisson's ratio was assumed to be equal to 0.3. The morphology of at the interface, located at 2 km depth [*Zollo et al.,* 1996] was considered flat in this work. The source geometry was chosen taking into account the tomography images and its resolution [*Capuano et al.,* 2003], as explained in the previous section. To obtain an adequate source volume we used a prolate parallelepiped shape, differently from Russo and Giberti [2004] that used prolate ellipsoidal or cylindrical shape. The shape size was also constrained by the number of elements and by the type of element (hexahedral).

For each model the three components of the ground deformation were computed at the nodes of FEM mesh, corresponding to the real topographic surface. A uniform overpressure of 10 MPa was applied to the source walls. Different overpressure values will affect the ground deformation magnitude but the deformation pattern will keep unchanged, due to the linear elastic material model used in the simulation.

4. Results and conclusion

Results relative to the source located at 2, 3 and 5 km are reported below for homogenous and heterogeneous medium.

4.1 Homogenous medium

The surface deformation produced by a source located at 2 km depth is shown in Figure 4a. A strong deviation from an axial symmetrical pattern of the displacement field is evident due to the presence of the real topography. As pointed out by *Lungarini et al.* [2005] at Etna volcano, the peculiar effect of real topography is to increase displacements at the point of lower elevation. Maxima are located on the slope of the volcano (Colle Umberto, Colle dei Canteroni and Cognoli di Trocchia area), while the maximum uplift is located in SE area. Deformation is concentrated in a radial distance of about 3 km from the crater axis. Another relevant characteristic is the presence of small area in subsidence at middle-high elevation, with a strong variability in the summit area. The

complex deformation pattern is still present when the source is located deeper, even if with a smaller amplitude. This is shown in Fig. 5a, b, where the deformation for each component and each source depth, along N-S and E-W profiles are plotted. To verify the effects of real topography we firstly computed the ground deformation produced by a Mogi model without topography and then by assuming an axial symmetrical shape of the volcano. The axial-symmetrical volcano was realized by rotating a simulated profile obtained considering a height of 1230m (maximum elevation of the volcano) and a constant slope to reach sea level at a distance of 5km (distance of the crater axis to the coast); the sources were located 3 km depth below sea level and their volume was equivalent (0.4 km^3 about).

Figure 6 shows the vertical and radial ground displacements for both simulations showing the complexity added by the real topography, which obviously decrease with the source depth. The Mogi model and also the simplified topography were not able to define the influence of the real topography and therefore they can provide incorrect localisation of the sources of the observed deformations and incorrect data to signal a possible volcano reawakening. The real topography produced also non-zero values of the NS component along EW direction and vice versa (Fig. 5a, b). The horizontal components of the deformation field show a complex pattern in the summit area, evidencing also some shortening areas.

4.2 Heterogeneous medium

The surface deformation produced by a source located at 2 km depth is shown in Figure 4b. Also in this case with the presence of a carbonate layer, the ground deformation is strongly affected by the topography with similar characteristics. Moreover, maximum vertical displacements are greater with respect to the homogeneous case in the crater region. In this case the source was located above and below the interface between the two layers (carbonate and volcanic coverage) and the differences in Young's modulus creates additional vertical forces in the area above the

source. In regions away from the crater axis, higher displacements were experienced by the model with homogenous material.

Sources located at greater depth showed similar behaviour with smaller amplitude. The maximum horizontal displacements show similar increased amplitude and coupling between the two horizontal components (Fig. 5c, d).

5. Conclusion

In a volcanic area, ground deformations are generally studied by using a simple models, taking into account both the topography and the heterogeneity of the medium. This approach can provide incorrect measured displacements and the deformation scenario when used in hazard analysis. Thus, simulation of the expected deformation pattern with a more complex model was needed. We started to investigate the influence of real topography at the most hazardous central volcano in the world: the Somma-Vesuvius structure. We performed simulations of overpressure sources whose geometry (shape, depth and lateral extension) were constrained mainly by results of seismic tomography studies carried out in the last ten years.

The main results of our simulation, performed using a real topography, was the presence of a strong deviation from the axial symmetrical deformation pattern, around the crater axis, with the peculiar effect of enhancing displacements at the point of lower elevation. This behaviour was also characterized by small subsidence areas and by the presence of non-zero horizontal component (x or y) along the orthogonal direction (y or x). Both these characteristics were completely unknown in the simple Mogi model and also by model created using simplified topography. These results can be very helpful in the understanding the position of the sources of ground deformation during volcano reawakening and for a better definition of the geometry and characteristic of a geodetic monitoring network, particularly in the summit area, that experienced strong deformation differences with respect to the simplified models.

For a more accurate modelling that could help in unbiased analysis of deformation produced by possible uplift events on the summit of Vesuvius, and in the definition of a more accurate monitoring network, further refinements of the model are needed. This will include a finer mesh, the introduction of the real morphology of a carbonate basement as shown by the tomography [*Zollo et al.,* 1996], a detailed description of the elastic characteristics of the volcanic coverage for an improved modelling of a complex elastic structure, the introduction of the bathymetry of the gulf of Naples, and finally the simulation of different pressure source shapes, compatible with the tomography constraints.

4. Acknowledgments

We are grateful to the Laboratorio di Geomatica e Cartografia (INGV-OV) for providing the DTM of the area. This work was partially funded by Istituto Nazionale di Geofisica e Vulcanologia and Dipartimento della Protezione Civile. The reviewer's comments improved strongly this paper.

References

Akaike H. (1974), A new look at the statistical model identification, *IEEE Trans. Autom. Contr.*, 6, 716-723.

Auger E., Gasparini P., Virieux J., Zollo A. (2001), Seismic evidence of an extended magmatic sill under Mt. Vesuvius, *Science*, *294*, 1510– 1512.

Belkin H. E. , De Vivo B. (1993). Fluid inclusion studies of ejected nodules from plinian eruptions at Mt.Vesuvius, *J. Volcanol. Geotherm. Res.*, 58, 89-100.

Capuano P., Gasparini P., Virieux J., Zollo A., Casale, R., Yeroyanni M. (eds.) (2003), *The Internal Structure of Mt. Vesuvius: A Seismic Tomography Investigation*, Liguori Editore, Napoli, pp.595, ISBN: 88-207-3503-2.

Cayol V., Cornet F. H. (1998), Effects of topography on the interpretation of the deformation field of prominent volcanoes, Application to Etna, *Geophys. Res. Lett.*, 25, n.11, 1979-1982.

De Matteis, R., Latorre, D., Zollo, A., Virieux, J., (2000). 1-D P-velocity models of Mt Vesuvius Volcano from the Inversion of TomoVes96 First Arrival Time Data, *Pageoph,* 157**,** 1643–1661.

De Natale G., Troise C., Trigila R., Dolfi D., Chiarabba C. (2004), Seismicity and 3-D substructure at Somma-Vesuvius volcano: evidence for magma quenching, *Earth and Planet. Sci. Lett.*, 221, 181-196.

Di Stefano R., Chiarabba C. (2002), Active source tomography at Mt. Vesuvius: Constraints for the magmatic system, *J. Geophys. Res.*, 107, 2278-2292.

Fulignati P., Marianelli P., Sbrana A. (2000). New insight on the thermometamorphic-metasomatic magma chamber shell of the 1944 eruption of Vesuvius, *Acta Vulcanol.*, 10, 47-54.

Gasparini and Tomoves working group (1998). Looking inside Mount Vesuvius, *EOS*, 79, n. 19, 229-232.

Goldberg X. (1989), Genetic algorithm, in *Search, optimization and machine learning*, Addison-Wesley Pub. Co., Boston.

Lomax A., Zollo A., Capuano P., Virieux J. (2001), Precise, absolute earthquake location under Somma-Vesuvius volcano using a new three-dimensional velocity model, *Geophys. J. Int,* 146, 2, 313-331.

Lungarini L., Troise C., Meo M., De Natale G. (2005), Finite element modelling of topographic effects on elastic ground deformation at Mt. Etna, *J. Volcanol. Geotherm. Res.,* 144, 257-271.

Lutter W.J., Nowack R.L. (1990), Inversion of crustal structure using reflections from the ASSCAL Ouachita experiment, *J. Geophys. Res.*, 95, 4633-4646.

McTigue D. F., Segall P. (1988), Displacements and tilts from dip-slip faults and magma chambers beneath irregular surface topography, *Geophys. Res. Lett., 15*, 601-604.

Mogi O. (1958), Relations between the eruptions of various volcanoes and the deformations of the ground surface around them., *Bull. Earthq. Res. Inst. Univ. Tokyo,* 36, 209-225.

Press W.H., Flannery B.P., Teukolsky S.A., Vetterling W.T. (1986), *Numerical recipes*, Cambridge Univ. Press, Cambridge.

Russo G., Giberti G. (2004), Numerical modeling of surface deformations on Mt. Vesuvius volcano (Italy) in presence of asymmetric elastic heterogeneities, *J. Volcanol. Geotherm. Res.,* 133, 41-54.

Tarantola, A., Valette, B., (1982). Inverse problems=quest for information, *J. Geophys*., 50, 159–170.

Trasatti E., Giunchi C., Bonafede M. (2003), effects of topography and rheological layering on ground deformation in volcanic regions, *J. Volcanol. Geotherm. Res.*, 122, 89-110.

Williams C. A., Wadge G. (1998), The effects of topography on magma deformation models: application to Mt. Etna and radar interferometry, *Geophys. Res. Lett. 25*, 1549-1552.

Zollo A., Gasparini P., Virieux J., Le Meur H., De Natale G., Biella G., Boschi E., Capuano P., De Franco R., Dell'Aversana P., De Matteis R., Guerra I., Iannaccone G., Mirabile L., Vilardo G. (1996), Seismic evidence for a low velocity zone in the upper crust beneath Mount Vesuvius. *Science,* 274, 592-594.

Zollo A., D'Auria L., De Matteis R., Herrero A., Virieux J. and Gasparini P. (2002). Bayesian estimation of 2-D P-velocity models from active seismic arrival time data: Imaging of the shallow structure of Mt. Vesuvius (Southern Italy), *Geophys. J. Int.*, 151, 566-582.

Figure captions and Table

Fig. 1 Sketch map of the Vesuvius volcanic area. The TomoVes shot points position (e.g. A1, B1, …) and the seismic stations locations are also shown. Shading indicates the topography (brown = higher elevations, corresponding to the Mesozoic Carbonate; green = lower elevations, corresponding to the Campanian Plain). The inset represents a zoom of the crater area.

Fig. 2 2D P-velocity model relative to 5 profiles. The dashed line delimitates at depth the best resolved areas as inferred from the checkerboard resolution tests. (Zollo at al., 2002)

Fig. 3 Finite Element model

Fig. 4 Homogeneous medium - Vertical displacements produced by a source located at 2 km depth (a); Heterogeneous medium -Vertical displacements produced by a source located at 2 km depth (b). Each map is normalized to the maximum value of the displacement, i.e. the maximum vertical displacement for the heterogeneous model.

Fig. 5 Normalized vertical and horizontal displacements profile with source located at 2 (black), 3 (dashed blue), 5 km (green) depth: (a) homogeneous case along South-North; (b) homogeneous case along West-East; (c) heterogeneous case along South-North; (d) heterogeneous case along West-East.

Fig. 6 Vertical (red) and radial (black) displacements for the Mogi model (dashed line) and an axisymmetric (continuous line) topography with a source located at 3 km depth. Displacements are normalized to the maximum value of vertical displacement with real topography.

Table 1. Boundary conditions.

Node position	Constrain
External faces with y=constant	Y direction
External faces with x=constant	X direction
Bottom	Z direction
Top	No

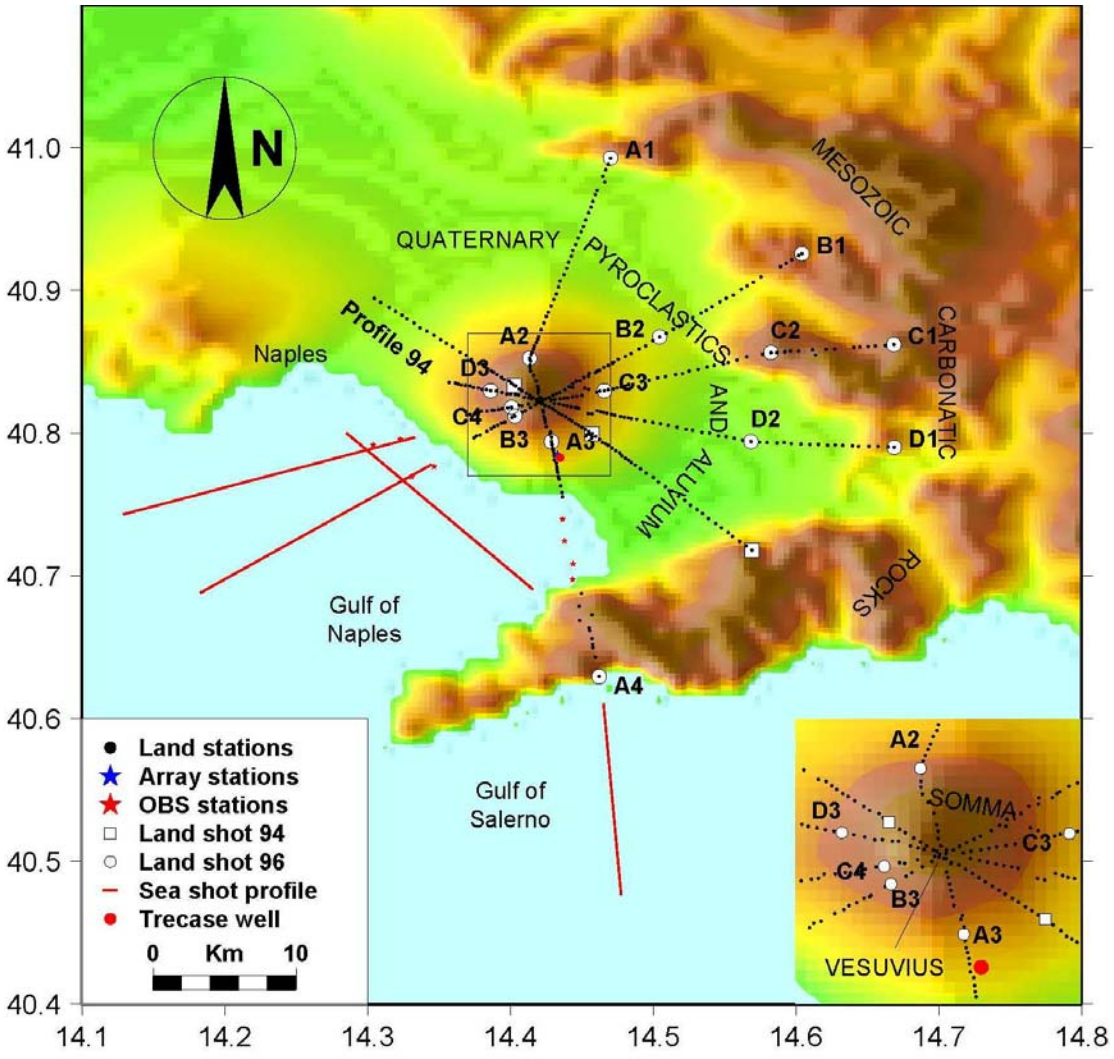

Figure 1

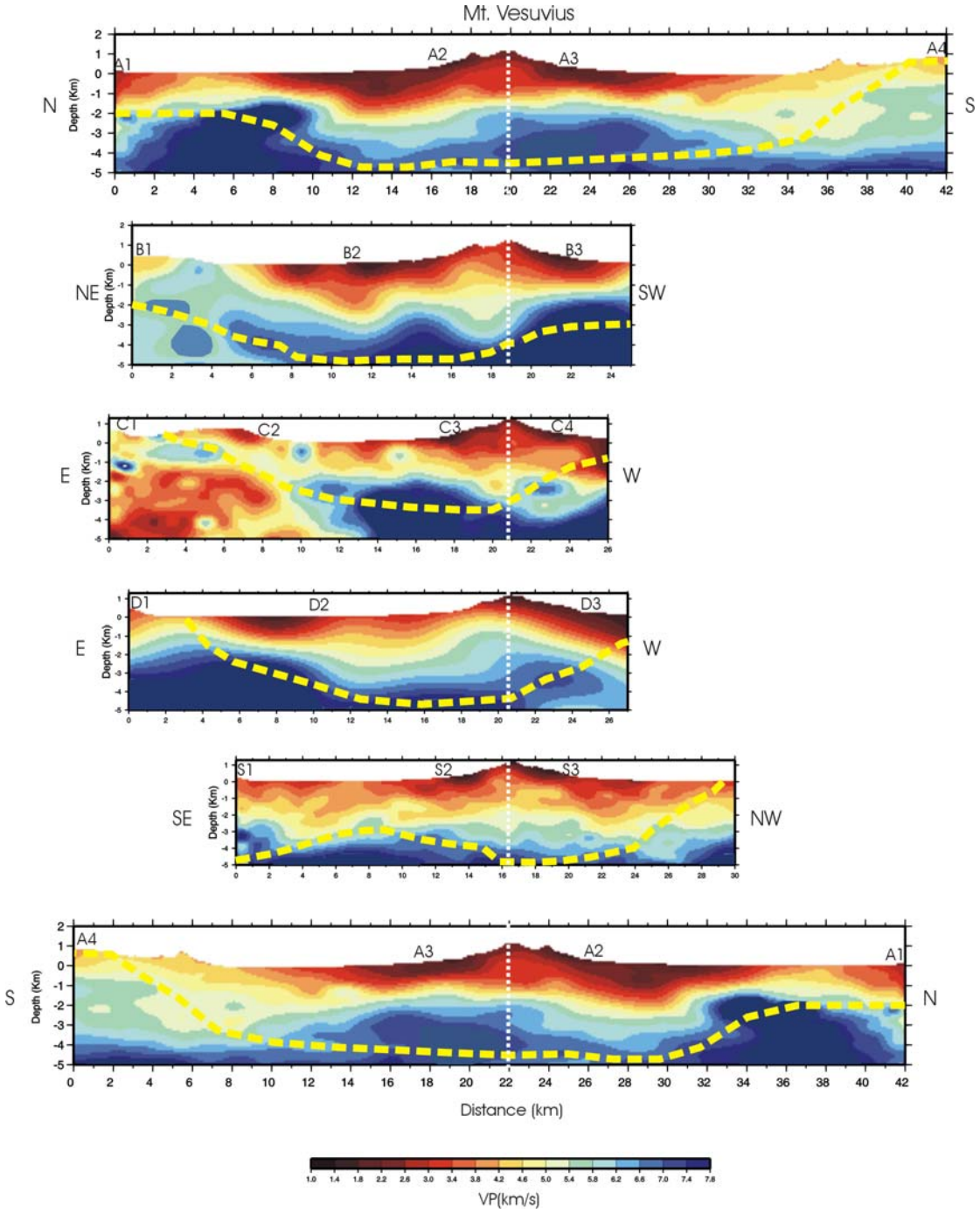

Figure 2

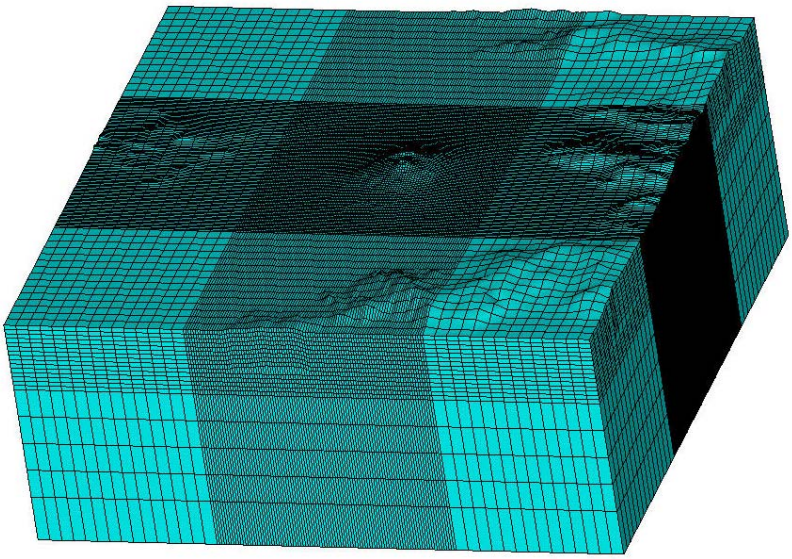

Figure 3

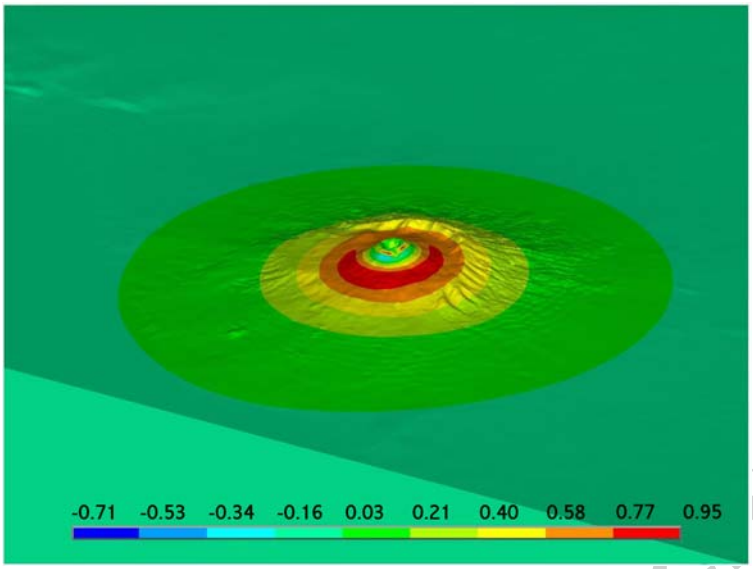

a)

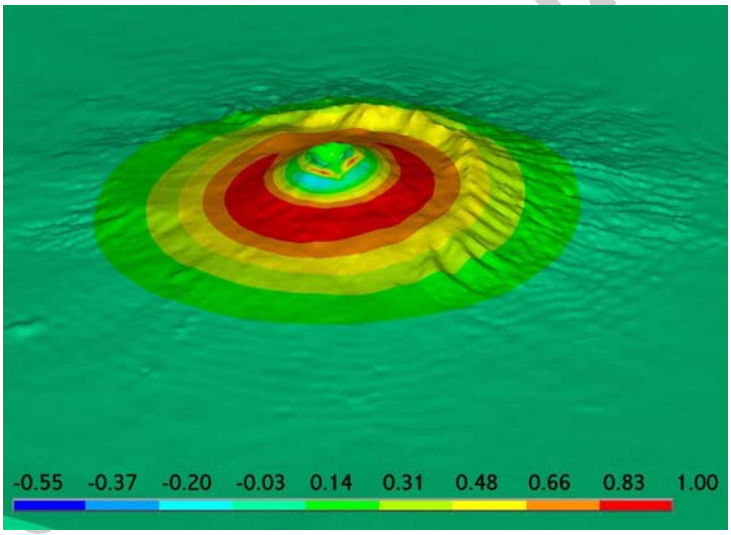

b)

Figure 4

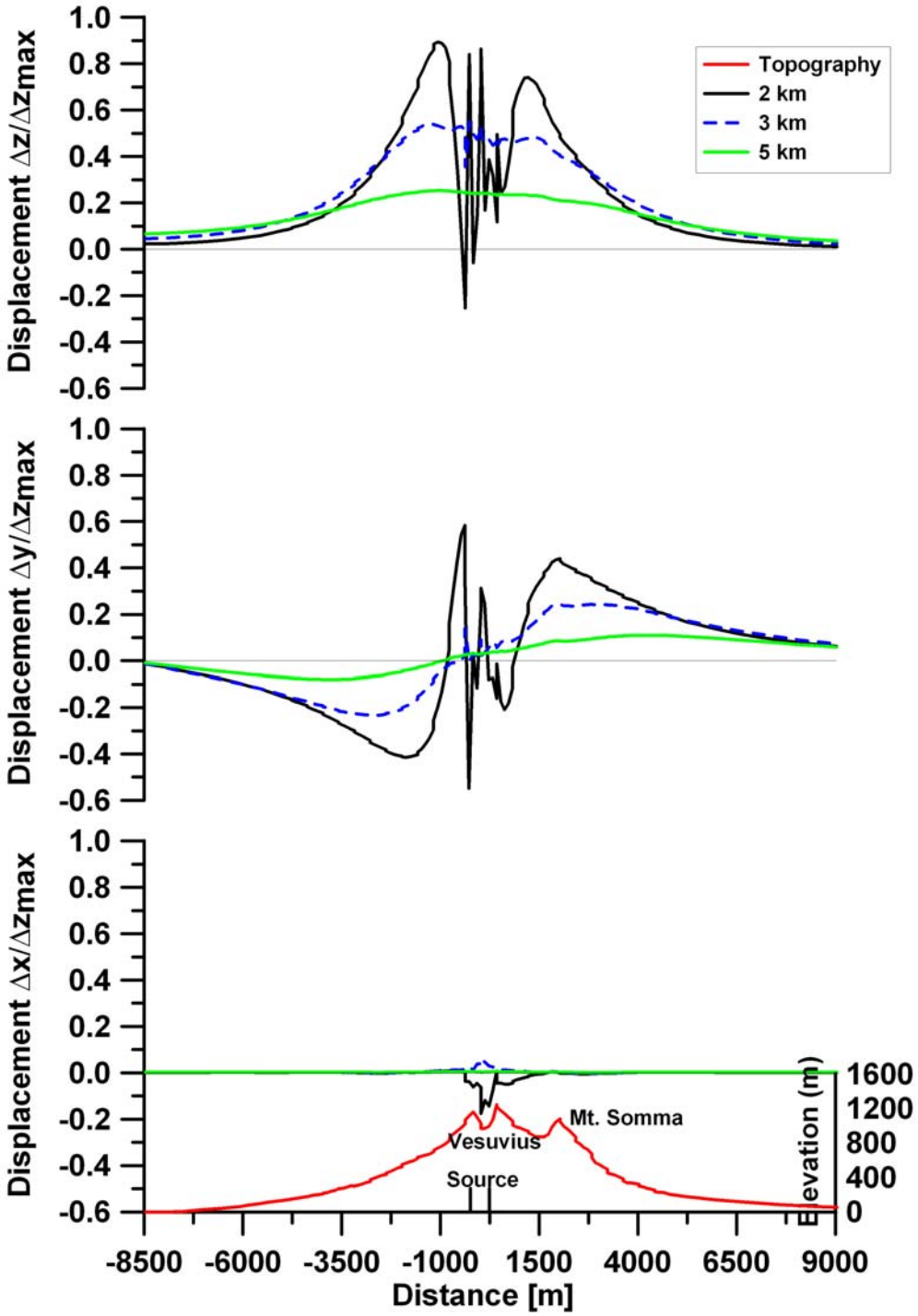

Figure 5a

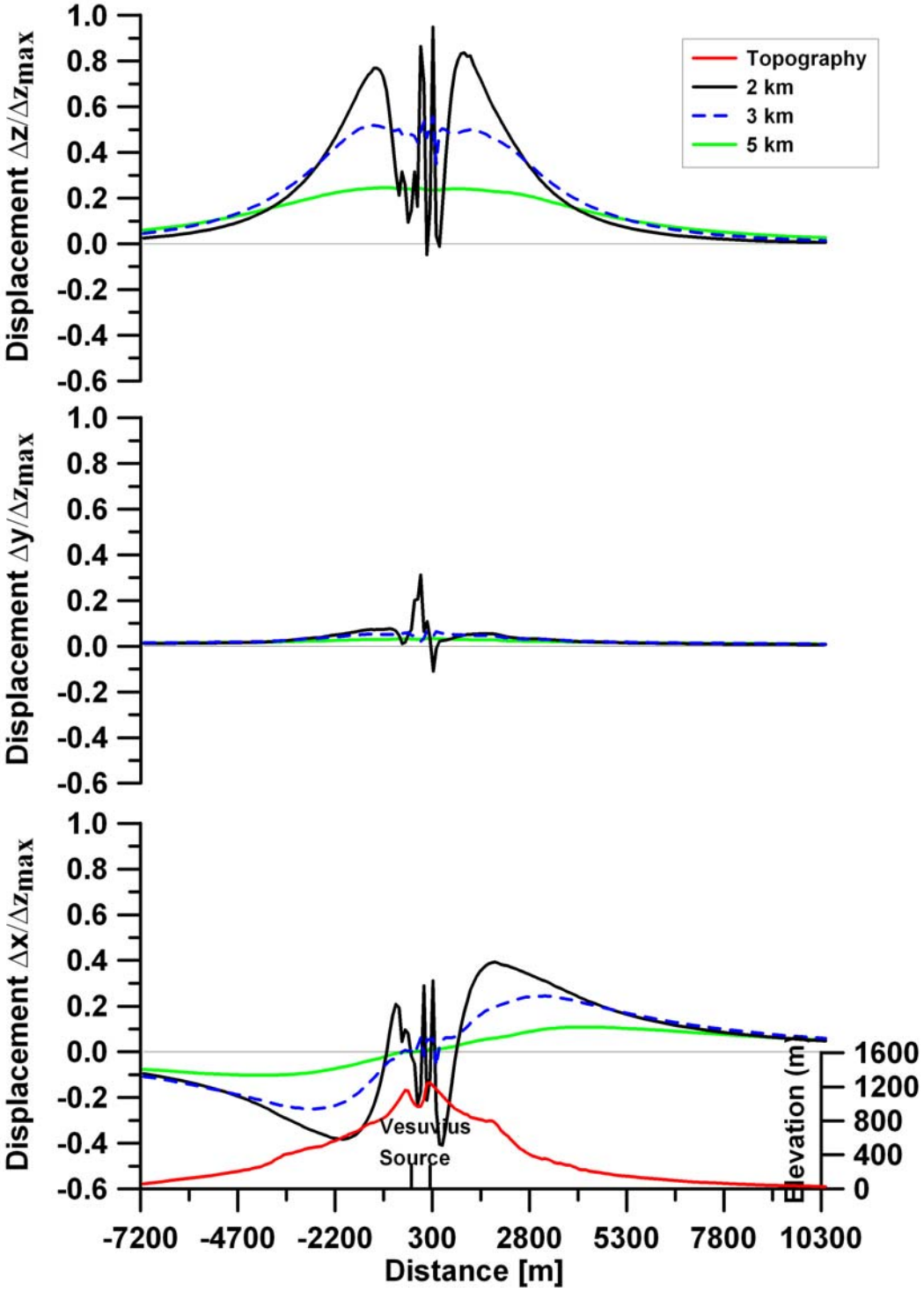

Figure 5b

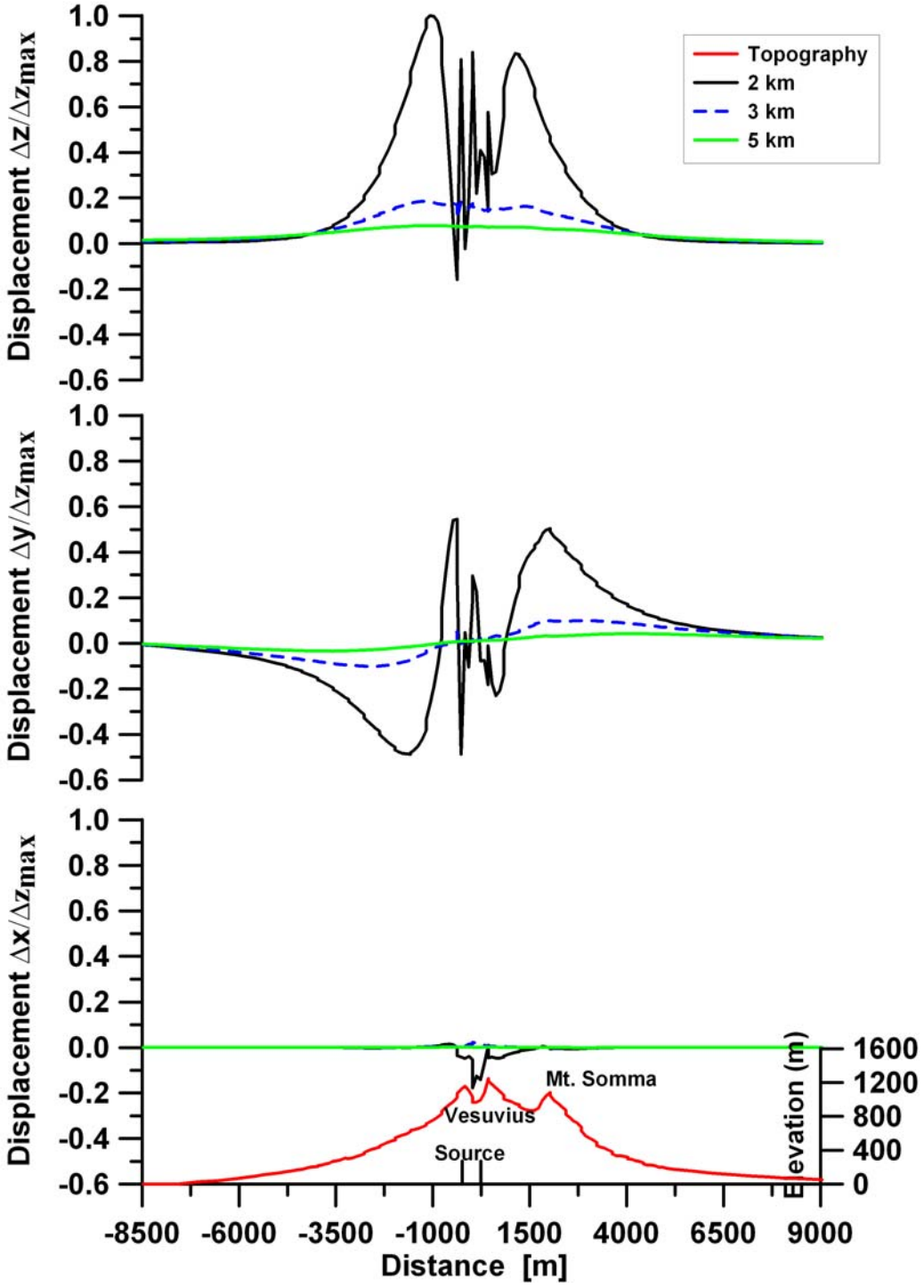

Figure 5c

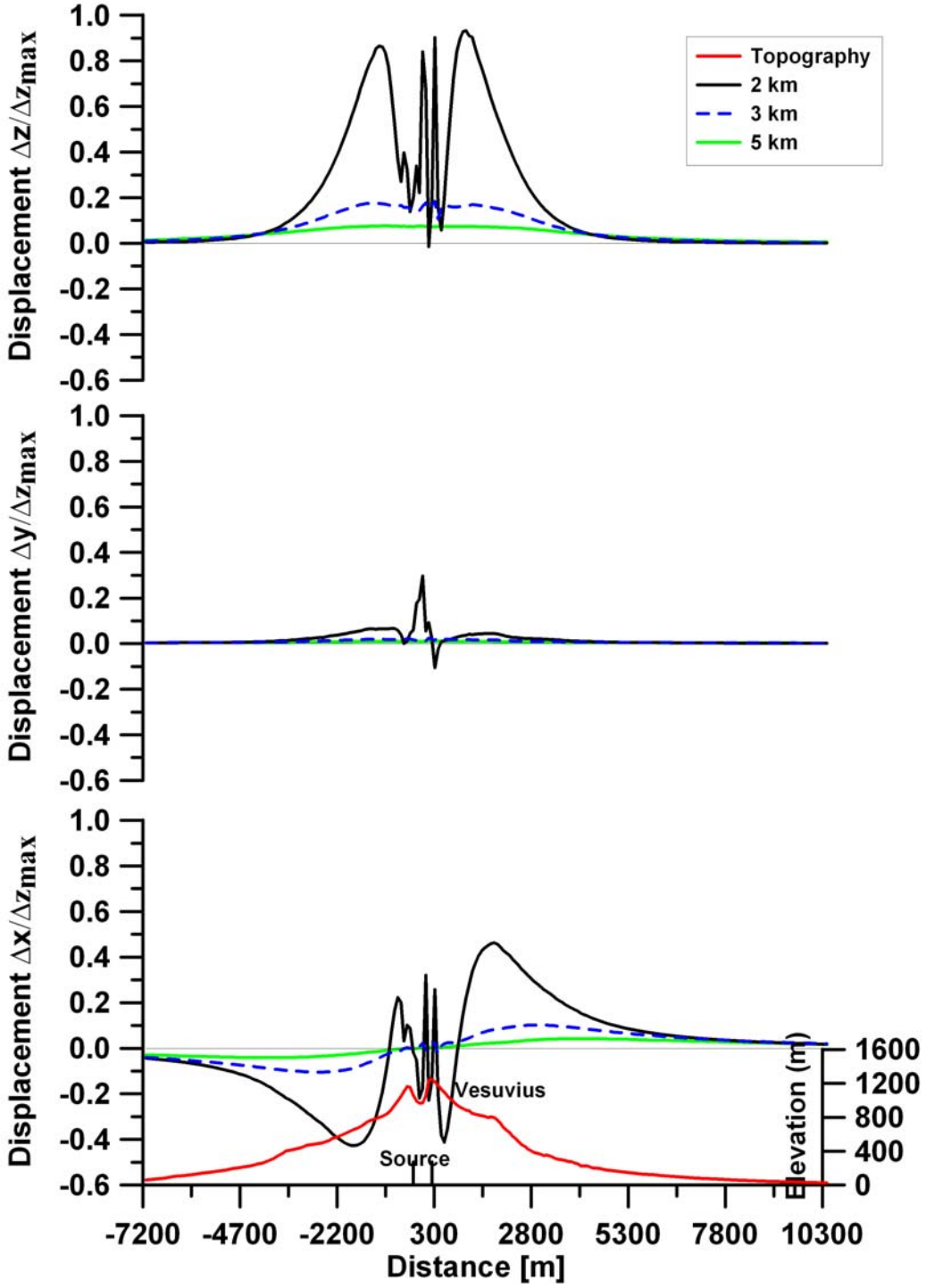

Figure 5d

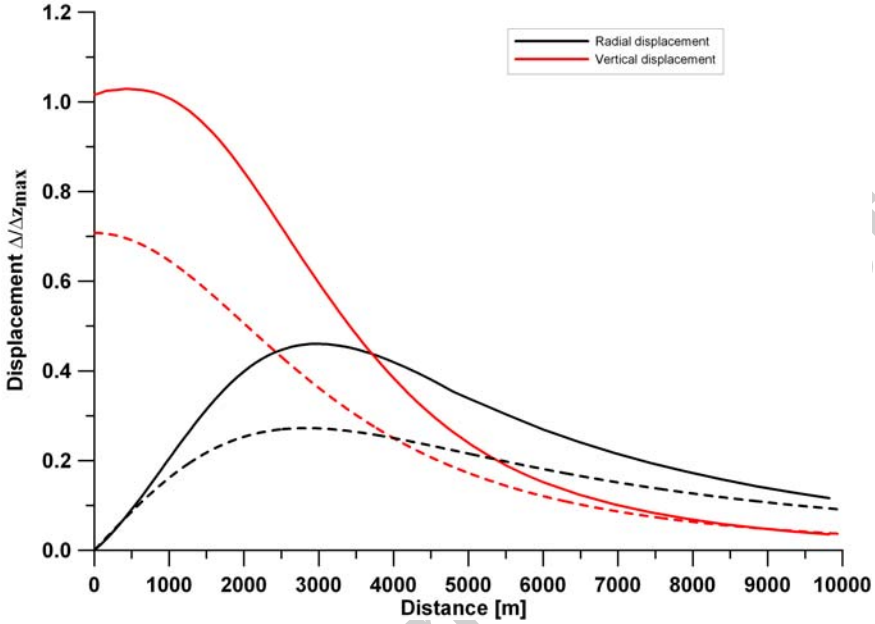

Figure 6